Oxidized LDL/CD36 interaction induces loss of cell polarity and inhibits macrophage locomotion

Young Mi Park[a,b,*], Judith A. Drazba[c,†], Amit Vasanji[d], Thomas Egelhoff[a,b], Maria Febbraio[b,e], and Roy L. Silverstein[a,b,†]

[a]Department of Cell Biology, [c]Imaging Core, [d]Biomedical Imaging and Analysis Core, and [e]Department of Molecular Cardiology, Lerner Research Institute, Cleveland Clinic, Cleveland, OH 44195; [b]Department of Molecular Medicine, Cleveland Clinic Lerner College of Medicine of Case Western Reserve University, Cleveland, OH 44195

ABSTRACT **Cell polarization is essential for migration and the exploratory function of leukocytes. However, the mechanism by which cells maintain polarity or how cells revert to the immobilized state by gaining cellular symmetry is not clear. Previously we showed that interaction between oxidized low-density lipoprotein (oxLDL) and CD36 inhibits macrophage migration; in the current study we tested the hypothesis that oxLDL/CD36-induced inhibition of migration is the result of intracellular signals that regulate cell polarity. Live cell imaging of macrophages showed that oxLDL actuated retraction of macrophage front end lamellipodia and induced loss of cell polarity. *Cd36 null* and macrophages null for *Vav*, a guanine nucleotide exchange factor (GEF), did not show this effect. These findings were caused by Rac-mediated inhibition of nonmuscle myosin II, a cell polarity determinant. OxLDL induced dephosphorylation of myosin regulatory light chain (MRLC) by increasing the activity of Rac. Six-thioguanine triphosphate (6-thio-GTP), which inhibits Vav-mediated activation of Rac, abrogated the effect of oxLDL. Activation of the Vav-Rac-myosin II pathway by oxidant stress may induce trapping of macrophages at sites of chronic inflammation such as atherosclerotic plaque.**

Monitoring Editor
Carole Parent
National Institutes of Health

Received: Dec 28, 2011
Revised: Apr 30, 2012
Accepted: Jun 13, 2012

INTRODUCTION

Cell polarization is a prerequisite for migration (Lauffenburger and Horwitz, 1996) and is mediated by interlinked molecular pathways (Ridley *et al.*, 2003). This intrinsically self-reinforcing mechanism results in generation of the protrusive front and retraction of the rear end, and thus maintains a certain degree of persistent directional cell movement even in the absence of external directionality cues (Zigmond *et al.*, 1981; Pankov *et al.*, 2005). For leukocytes, exploratory locomotion driven by spontaneous breakage of cellular symmetry enables cells to sense the surrounding environment and is critical for the propagation of immune and inflammatory responses (Parent and Devreotes, 1999; Vicente-Manzanares and Sánchez-Madrid, 2004). Mechanisms underlying spontaneous cell polarization, however, are not clearly defined. The ability of cells to spontaneously generate asymmetry is linked to mechanisms by which cells maintain symmetry and remain stationary. Therefore elucidating the process in which cells lose polarity may help identify key mediators of the polarization process.

Rho family small-molecular-weight guanine triphosphatases (GTPases) are known to play a role in cell polarization by regulating cytoskeletal dynamics (Nobes and Hall, 1999; Wittmann and Waterman-Storer, 2001; Raftopoulou and Hall, 2004). Rac generates protrusive force at the leading edge by regulating polymerization of actin, and RhoA is involved in retraction of the rear end. Cytoskeletal regulation by Rho GTPases is complex because of a network of interacting molecules including guanine-nucleotide exchange factors (GEFs), GTPase-activating proteins, scaffold proteins including Wiskott-Aldrich syndrome proteins (WASPs), WASP family verprolin-homologous proteins, and phosphoinositide-3 kinase (Charest and

This article was published online ahead of print in MBoC in Press (http://www.molbiolcell.org/cgi/doi/10.1091/mbc.E11-12-1051) on June 20, 2012.

Present address: *Department of Molecular Medicine, Ewha Womans University School of Medicine, Seoul 158-710, Republic of Korea; †Department of Medicine, Medical College of Wisconsin, Milwaukee, WI 53226.

Address correspondence to: Roy L. Silverstein (rsilverstein@mcw.edu).

Abbreviations used: 6-thio-GTP, 6- thioguanine triphosphate; FAK, focal adhesion kinase; GEF, guanine nucleotide exchange factor; MCP-1, monocyte chemotaxis protein-1; MLCK, myosin light chain kinase; MP, myosin phosphatase; MPO, myeloperoxidase; MRLC, myosin regulatory light chain; oxLDL, oxidized low-density lipoprotein; PAK, p21-activated kinase; RNAi, RNA interference; ROK, Rho kinase; *wt*, wild type.

Firtel, 2007). Interplay among different Rho GTPases can also produce compound effects on the cytoskeleton (Sander *et al.*, 1999; Yamaguchi *et al.*, 2001). Cells expressing a dominant-negative Rac1 have defects in pseudopodia protrusion and generation of F-actin–rich leading edges, resulting in poor motility (Chung *et al.*, 2000). Significantly, cells expressing constitutively active forms of Rac are also defective in motility, suggesting the importance of balanced regulation of interlinked pathways (Chung *et al.*, 2000; Dumontier *et al.*, 2000). Nonmuscle myosin II is regulated by Rho GTPases and also mediates cytoskeletal dynamics (Zhao and Manser, 2005). The activity of nonmuscle myosin II depends on the reversible phosphorylation of the myosin regulatory light chain (MRLC) on Ser-19 (Somlyo and Somlyo, 2003) and is further increased by additional phosphorylation of Thr-18 of MRLC in the presence of phosphorylated Ser-19 (Ikebe *et al.* 1986). RhoA activates nonmuscle myosin II by inhibiting myosin phosphatase (MP), thereby increasing phosphorylation of MRLC (Amano *et al.*, 1996; Kimura *et al.*, 1996; Kawano *et al.*, 1999). Rac promotes contractility by activating p21-activated kinase (PAK), which directly phosphorylates MRLC (Chew *et al.*, 1998). However, there are contradictory findings about the effect of Rac on myosin II, because Rac signaling is also implicated in the negative regulation of myosin by promoting actin–myosin disassembly (van Leeuwen *et al.*, 1999). In addition, activated PAK phosphorylates and inhibits myosin light chain kinase (MLCK) (Sanders *et al.*, 1999; Goeckeler *et al.*, 2000). To date, all studies on the roles of Rho GTPases in cell polarization have used dominant negative mutants or introduced constitutively active forms that may have driven these contradictory effects. No studies have been published showing that these pathways can be perturbed endogenously to drive pathological processes.

Our lab has a long-standing interest in CD36, a transmembrane glycoprotein receptor expressed in a variety of cells including monocytes and macrophages. CD36 promotes atherosclerosis by mediating oxidized low-density lipoprotein (oxLDL) uptake in macrophages leading to the formation of lipid-laden foam cells (Febbraio *et al.*, 2000, 2004; Rahaman *et al.*, 2006; Guy *et al.*, 2007; Kuchibhotla *et al.*, 2008). CD36 also inhibits macrophage migration (Park *et al.*, 2009) and thus contributes to foam cell accumulation in the vascular intima, leading to development of atherosclerotic plaque. We and others have hypothesized that strategies to promote lipid-laden macrophage egress from the vessel wall may be useful to prevent or reverse atherosclerosis, and indeed several studies have shown that regressed atherosclerotic plaque is characterized by the disappearance of foam cells (Daoud *et al.*, 1981; Llodra *et al.*, 2004) associated with their emigration to regional lymph nodes (Llodra *et al.*, 2004).

In the current study we tested the hypothesis that oxLDL/CD36 interactions inhibit migration as a result of intracellular signals that regulate cell polarity. We showed that Rac1 activation by Vav family GEFs induced retraction of front end lamellipodia and loss of cell polarity in macrophages and found that interaction of oxLDL with CD36 triggered this pathway, leading to inactivation of nonmuscle myosin II through inhibition of phosphorylation of MRLC. These studies suggest that endogenous "danger signals" generated by oxidant stress can inhibit macrophage motility and provide a mechanistic explanation for altered migratory function of macrophages within atherosclerotic plaque and other inflammatory milieu containing oxLDL. The CD36–nonmuscle myosin II pathway could thus be a target for development of novel strategies to promote regression of atherosclerosis. Our data also describe a novel integrated paradigm for the mechanism of cell polarization that is modulated by a link between the Vav/Rac pathway and nonmuscle myosin II.

RESULTS

OxLDL inhibits murine macrophage locomotion by inducing loss of cell polarity

Live cell imaging showed that resident peritoneal macrophages from wild-type C57BL/6 (*wt*), *cd36* null, and *vav1* null mice plated on serum-coated glass coverslips made protrusions and then spontaneously polarized. Polarized macrophages protruded broad lamellipodia on their front ends and started to move by retracting their rear ends, leaving retraction fibers at the rear (Figure 1A; Supplemental Video 1). After the addition of NO_2LDL, a form of oxLDL modified by a myeloperoxidase (MPO)-nitrite system that is a specific ligand for CD36 (Podrez *et al.*, 1999), *wt* macrophages retracted their front end lamellipodia and generated retraction fibers around the front end, thus losing their polarity as well as their ability to advance (Figure 1A; Supplemental Video 2). Macrophages from *cd36* null mice did not show these changes and thus maintained the ability to migrate in the presence of NO_2LDL (Figure 1B; Supplemental Video 3). Similarly, macrophages from mice null for Vav1, a GEF recently shown to be a downstream effector of CD36 (Wilkinson *et al.*, 2006, Rahaman *et al.*, 2011), did not show lamellipodial retraction in response to NO_2LDL (Figure 1C; Supplemental Video 4).

Quantitative analysis of the live cell imaging studies was performed using several different parameters. NO_2LDL increased the number of retraction fibers per cell by 1.5-fold in *wt* macrophages but not in *cd36* null or *vav1* null cells (Figure 2, A and B). Dynamic movement of the macrophage membrane, assessed by measuring ruffle area, was decreased by NO_2LDL in *wt* but not *cd36* null macrophages (Figure 2, A and C; Supplemental Videos 5 and 6). NO_2LDL-induced changes were limited to the cellular front; ruffle area was not changed in the rear (Supplemental Figure S1). The response in *vav1* null cells was intermediate (Figure 2C). Macrophage velocity, measured as travel distance in 1 h, was decreased by NO_2LDL in *wt* but not *cd36* null or *vav1* null cells (Figure 2D). Thioglycollate-elicited macrophages behaved similarly to resident macrophages in this system (Supplemental Figure S2, A and B). In all studies, NO_2(–)LDL, a control LDL that was exposed to all the components of the MPO system except the oxidant, had no effect (Figure 2, E and F). These studies, in sum, showed that NO_2LDL inhibited directional cell movement in macrophages via a CD36-Vav–dependent mechanism.

OxLDL-induced inhibition of macrophage migration depends on CD36 and Vav family GEFs

We performed scratch wound closure assays combined with time-lapse microscopy to assess the effect of oxLDL-induced loss of polarity on macrophage migration. As shown in the representative image in Figure 3A, after 19 h, *wt* cells migrated into and completely filled the scratched cell-free space. As reported previously, migration of *vav1* null macrophages was slower than *wt* under basal conditions (Wells *et al.*, 2005; Spurrell *et al.*, 2009), and, as we reported previously (Park *et al.*, 2009), NO_2LDL treatment inhibited macrophage migration of *wt* but not *cd36* null cells by 50% (Figure 3, A and B). NO_2LDL treatment had significantly less impact on migration of *vav1* null macrophages compared with *wt* (Figure 3C). Because macrophages also express Vav3 (Sindrilaru *et al.*, 2009), we tested *Vav1,3* double-null macrophages and found that, like *cd36* null cells, *Vav1,3* double-null macrophages were not inhibited by NO_2LDL (Figure 3D). The bar graphs in Figure 3E show quantitative data from multiple migration experiments.

We also performed a modified Boyden chamber migration assay to see whether this effect of oxLDL inhibits chemoattractant-directed migration of macrophages. We placed murine macrophages with or

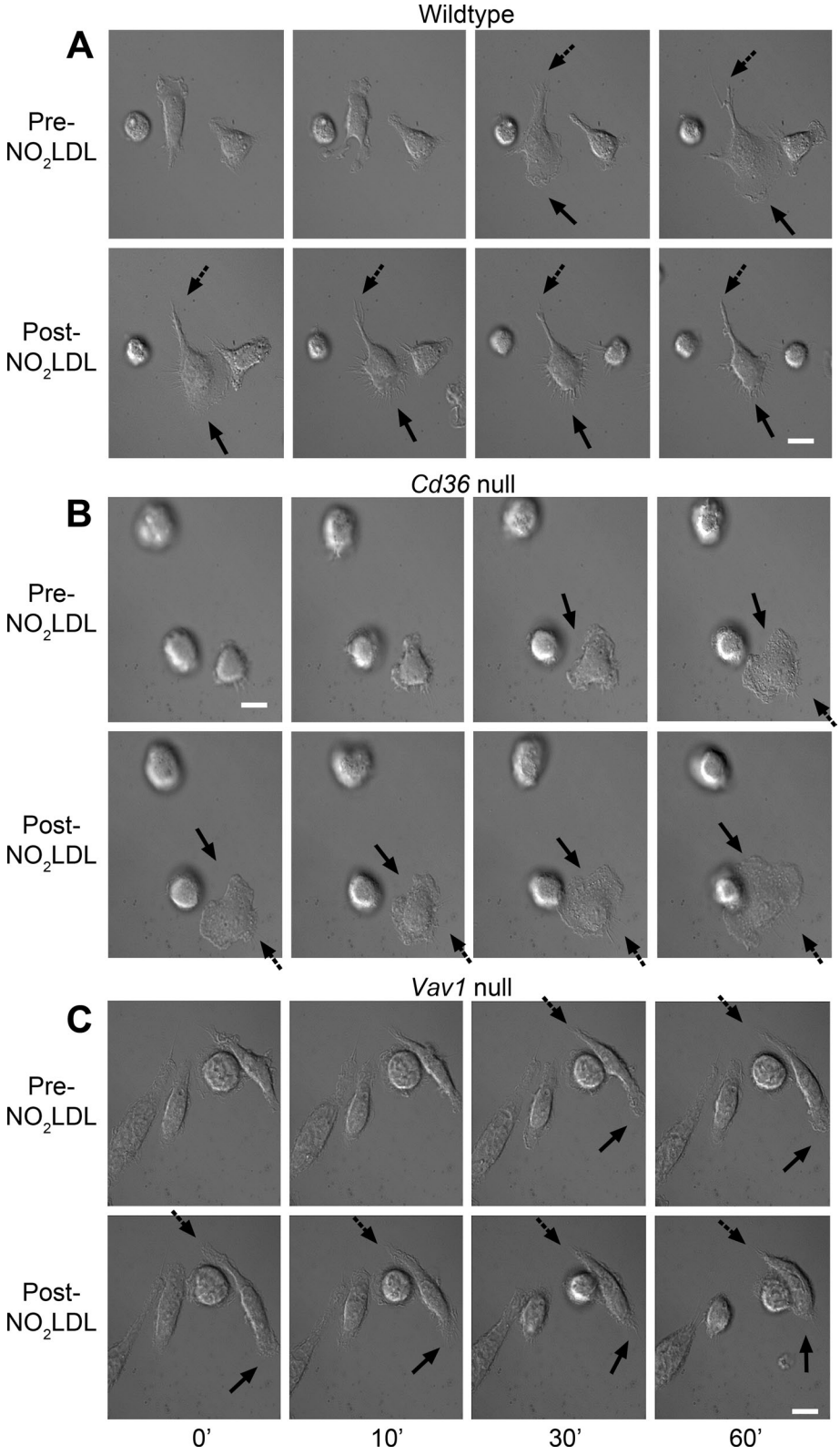

FIGURE 1: OxLDL induces retraction of lamellipodia and loss of cell polarity. (A) Resident peritoneal macrophages from *wt* mice were plated onto a serum-coated, glass bottom dish and allowed to spontaneously polarize. Time-lapse images were taken every 15 s for 1 h before and after the addition of NO_2LDL (50 μg/ml). Solid arrows indicate the front end lamellipodia, and dashed arrows indicate the rear end. Macrophages from *cd36* null mice (B) and *vav1* null mice (C) were tested as described in (A). Data are representative of five separate experiments analyzing 10–15 cells for each cell type. White scale bar = 10 μm.

without NO_2LDL onto the upper chamber and allowed migration toward the lower chamber containing monocyte chemotaxis protein-1 (MCP-1). Macrophage migration was facilitated by 1.4-fold when MCP-1 at 20 ng/ml was placed in the lower chamber. NO_2LDL treatment inhibited MCP-1–directed migration of *wt* macrophages but not that of *cd36* null cells and *vav1* null cells (Figure 3F).

OxLDL induces MRLC dephosphorylation

To evaluate mechanisms by which NO_2LDL induced lamellipodial retraction and loss of cell polarity, we determined the effect of NO_2LDL on activity of nonmuscle myosin II, a cell polarity determinant that is required to generate lamellipodial traction force (Phillips *et al.*, 2005; Vicente-Manzanares *et al.* 2007). Western blot assays to detect activating phosphorylation of T18/S19 in MRLC (Ikebe and Hartshorne, 1985; Ikebe *et al.*, 1988) showed that NO_2LDL treatment decreased the levels of phosphorylation by 60% in *wt* cells but not in macrophages from *cd36* null or *vav1* null mice (Figure 4A; $n = 8$, $p < 0.05$). NO_2LDL also induced a 60% decrease in phosphorylation of MRLC in human peripheral blood monocyte–derived macrophages. This decrease was blocked by an inhibitory anti-CD36 monoclonal antibody and was not observed using NO_2(–) LDL control (Figure 4, B and C).

Nonmuscle myosin II has three different heavy chain isoforms, IIa, IIb, and IIc, and leukocytes are generally known to express myosin IIa (Simons *et al.*, 1991). To determine which isoform is most affected by NO_2LDL, we assessed specific isoform expression by Western blot and found that macrophages expressed high levels of nonmuscle myosin IIa and low levels of IIb (Figure 4D). No differences were observed comparing *wt* to *cd36* null cells. We thus concluded that the cytoskeletal changes derived from myosin inactivation in macrophages were likely due to perturbed function of myosin IIa.

The small-molecular-weight G protein, Rac, is activated by oxLDL

To evaluate the mechanism by which MRLC dephosphorylation was induced by NO_2LDL, we used enzyme-linked immunosorbent assays (ELISAs) to detect the active GTP-bound forms of Rac and RhoA, and showed a dynamic increase in GTP-bound Rac in *wt*, but not in *cd36* null or *vav1* null macrophages after exposure to NO_2LDL (Figure 5A). GTP-bound RhoA was not affected by NO_2LDL (Figure 5B), nor was the

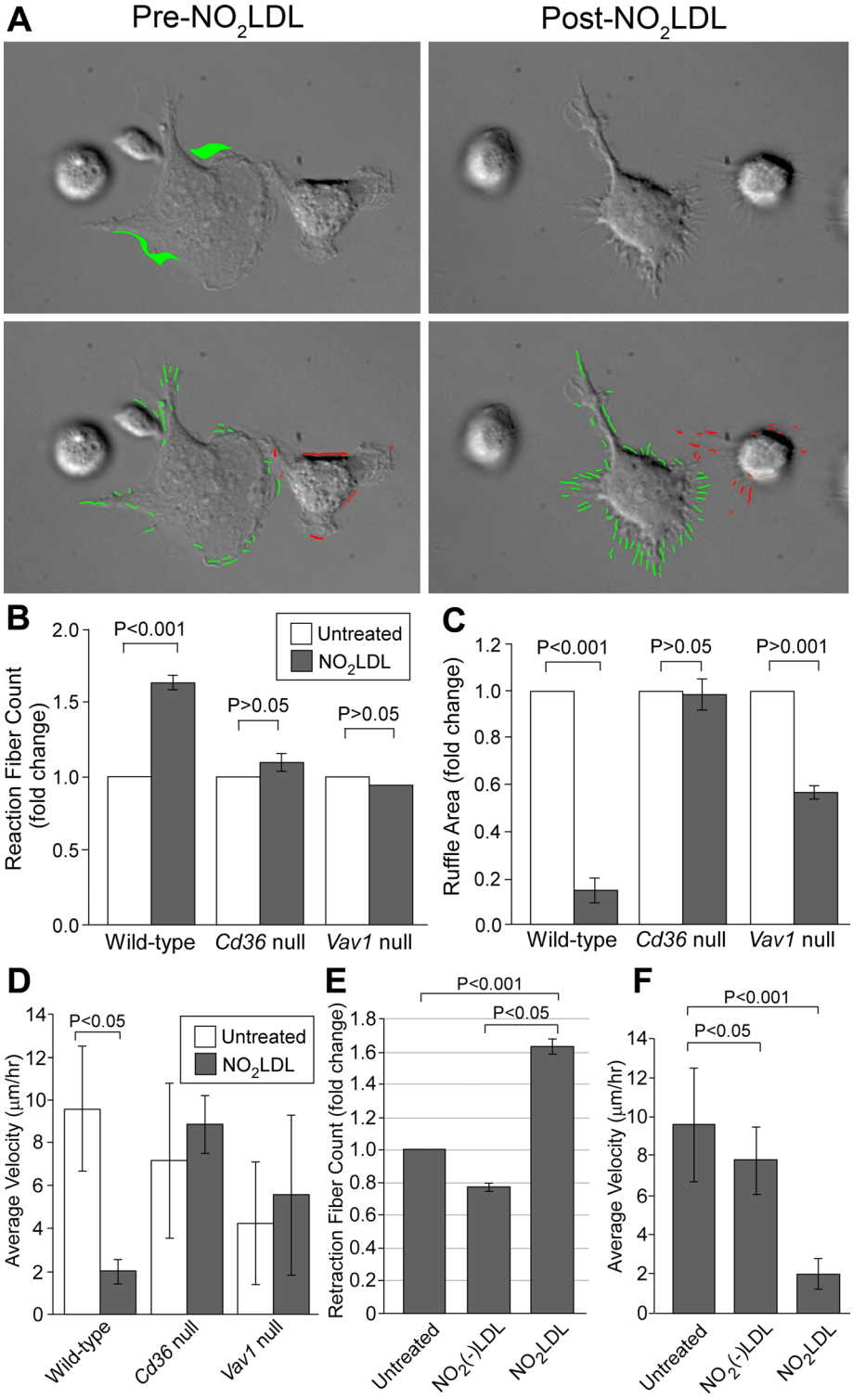

FIGURE 2: OxLDL induced retraction fiber formation around lamellipodia and decreased ruffle formation of macrophages. (A) Images from the time-lapse microscopy described in Figure 1 were analyzed with Image-Pro software (Media Cybernetics). Green or pink indicator lines were used to mark protrusions (top panels). The area in green is the newly formed protrusion from the prior cell margin imaged 15 s earlier (bottom panels). White scale bar = 10 μm. (B) Retraction fiber counts and (C) ruffle area were compared among *wt*, *cd36* null, and *vav1* null macrophages. (D) Velocity measured as travel distance in 1 h was compared among *wt*, *cd36* null, and *vav1* null macrophages. (E and F) *Wt* macrophages were treated with NO_2LDL or NO_2(–)LDL at 50 μg/ml as in Figure 1, and retraction fiber count (E) and velocity (F) were measured. (A–D) Data are representative of five separate experiments analyzing 10–15 cells for each cell type. (E and F) Data are representative of three separate experiments analyzing 9–12 cells for each treatment.

level of phosphorylated myosin binding subunit (Supplemental Figure S3), a downstream substrate for active RhoA (Ito *et al.*, 2004). We also performed immunoprecipitations of macrophage cell lysates with anti-Rac antibody to assess the physical association of Vav and Rac. Figure 5C shows that anti-Rac antibody coprecipitated Vav and that NO_2LDL treatment increased the amount of Vav coprecipitated by twofold within 2 min ($n = 3$, $p = 0.18$).

OxLDL inhibits myosin activity through Rac-mediated inhibition of MLCK

We used a pharmacological approach to confirm that NO_2LDL inactivated nonmuscle myosin II by activating Rac. As shown in the model in Figure 6A, calyculin-A is a myosin activator that increases MRLC phosphorylation by inhibiting MP (Kato *et al.*, 1986; Takai *et al.*, 1987; Ito *et al.*, 2004), thus bypassing the effect of myosin inhibitors such as Y27632 that act upstream of the phosphatase by inhibiting Rho and/or Rho kinase (ROK) (Shabir et al., 2004). Calyculin A, however, does not block myosin inhibitors such as ML-7 that act through the MLCK pathway (Fazal *et al.*, 2005). We thus incubated macrophages from *wt* mice with NO_2LDL in the presence or absence of calyculin-A. Western blot (Figure 6B; Supplemental Figure S4) showed that calyculin-A did not block the MRLC dephosphorylating effect of NO_2LDL (black arrow). As expected, it did block the effect of Y27632 (gray arrow) but not ML-7 (white arrow). Calyculin-A did not affect the level of phosphorylated MRLC by itself (Supplemental Figure S4). These results suggest that the activity of NO_2LDL is most likely mediated by inhibition of the MLCK pathway, as would be expected of an agent that activates Rac. MLCK is known to be inactivated by phosphorylation of its residues of Ser-439 and Ser-991 by PAK, a downstream effector of Rac (Goeckeler *et al.*, 2000; Lei *et al.*, 2000). Western blots showed that macrophages indeed had higher levels of phosphorylated (Ser-439) MLCK after exposure to NO_2LDL (Figure 6C), confirming that an NO_2LDL-induced signaling pathway inhibits myosin light chain phosphorylation through inactivation of MLCK.

Blocking oxLDL-induced Rac activation by 6-thioguanine triphosphate (6-thio-GTP) or RNA interference (RNAi) results in nonmuscle myosin II inhibition

We next evaluated whether inhibition of Rac activation blocked the inhibitory effect of NO_2LDL on MRLC phosphorylation.

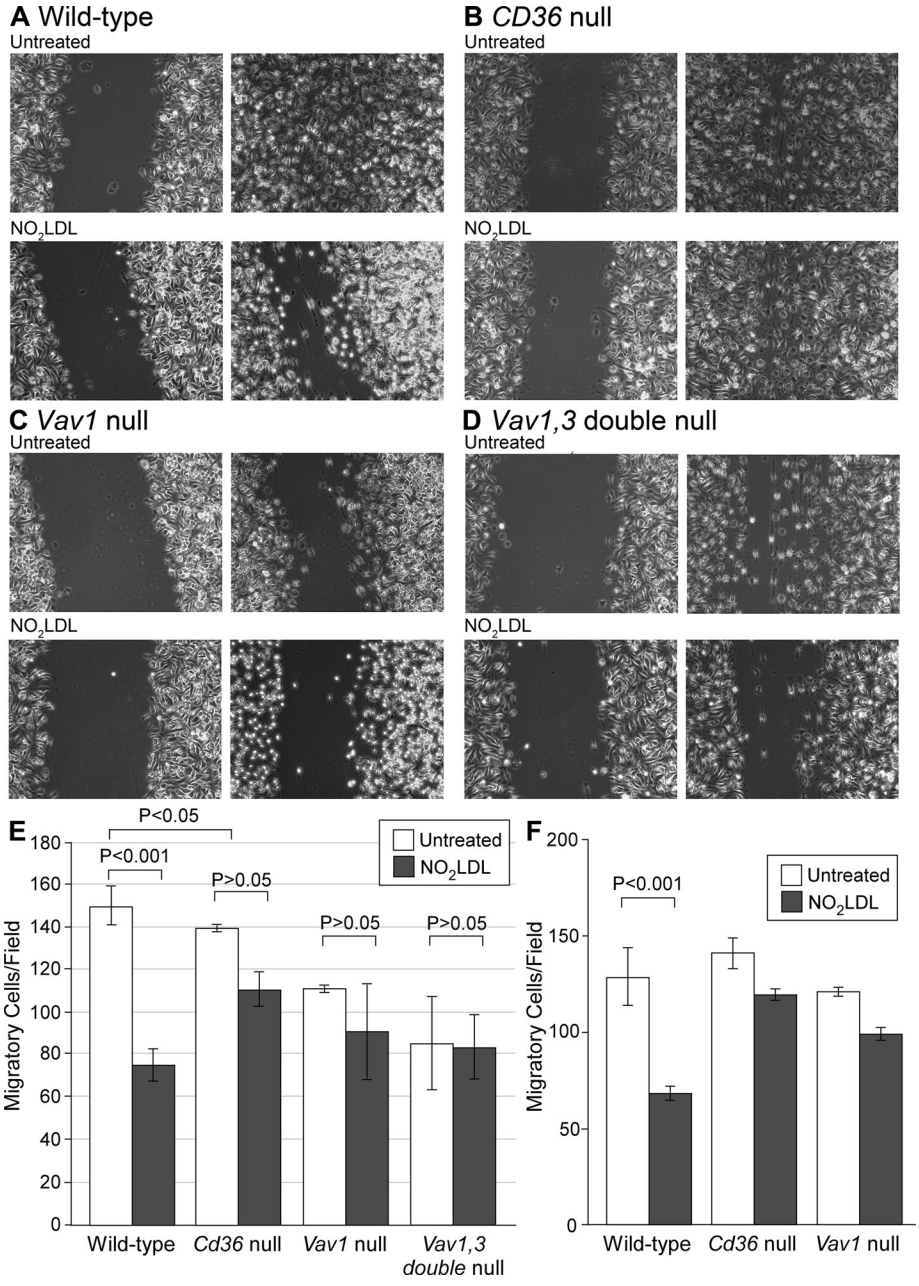

FIGURE 3: CD36-dependent inhibition of macrophage migration by oxLDL requires Vav family GEFs. Macrophages from *wt* (A), *cd36* null (B), *vav1* null (C), *or vav1,3* double-null (D) mice were plated onto a glass bottom dish. After 18 h, the confluent cell layer was scratched and treated with NO_2LDL or control LDL at 50 μg/ml. Macrophages migrating into the free space were counted after 19 h (right panels). (E) Quantitative analysis of migrated cells. Open bars are untreated macrophages, and filled bars are NO_2LDL-treated macrophages. Lines indicate SD. Data are representative of three separate experiments. In every experiment, three randomly chosen fields were recorded by time-lapse microscopy. (F) Macrophages from *wt*, *cd36* null, and *vav1* null mice were added to the upper chamber of the transwell with or without NO_2LDL (50 μg/ml) and were allowed to migrate through the porous membrane into the lower chamber containing medium with MCP-1. Migrated cells on the lower side of the membrane stained with DAPI were counted under a fluorescence microscope (100× magnification) and compared.

Six-thio-GTP, a metabolite of azathioprine, is an inhibitor that blocks Vav binding to Rac (Poppe *et al.*, 2006). Macrophages pretreated with 6-thio-GTP did not show an increase in GTP-bound Rac after NO_2LDL exposure (Figure 7A). Furthermore, Western blots for phosphorylated (Ser-19) MRLC showed that NO_2LDL failed to inhibit phosphorylation of MRLC in 6-thio-GTP pretreated macrophages (Figure 7, B and C). The inhibitory effect of 6-thio-GTP was time dependent; 4-h incubation incompletely blocked the effect of NO_2LDL; however, 16 h of incubation completely blocked it (Figure 7C). Sixteen-hour incubation with 6-thio-GTP did not affect cell viability; this finding was verified by trypan blue exclusion and Annexin V staining. Macrophages were also incubated with NSC23766, a Rac inhibitor that does not influence Vav but inhibits binding of alternative GEFs, including Tiam-1 and Trio (Gao *et al.*, 2004). Unlike 6-thio-GTP, NSC23766 did not block the effect of NO_2LDL on Rac activation (Figure 7A) or block the inhibitory effect of NO_2LDL on MRLC phosphorylation, further supporting a key role for Vav in NO_2LDL-induced inhibition of nonmuscle myosin II (Figure 7B).

We also confirmed the role of Rac in NO_2LDL-mediated inhibition of MRLC phosphorylation by using RNAi to knock down Rac1 expression in macrophages. The Rac1 RNAi down-regulated Rac1 protein expression by 54% (Supplemental Figure S5A) compared with a scrambled sequence control RNA. Western blot for phosphorylated (Ser-19) MRLC showed that NO_2LDL decreased the level of phosphorylated (Ser-19) MRLC in control macrophages, whereas it did not in the cells treated with the RNAi (Supplemental Figure S5B). Thus we conclude that Rac1 was required for inhibition of phosphorylation (Ser-19) of MRLC by NO_2LDL.

Six-thio-GTP blocks the effect of oxLDL on cell polarity and restores macrophage migration

Having shown that 6-thio-GTP blocks the biochemical signaling effects of NO_2LDL on Rac activation and MRLC phosphorylation, we next used live cell imaging to evaluate its effects on NO_2LDL-induced loss of cell polarity. Six-thio-GTP did not influence spontaneous polarization or locomotion of macrophages (Figure 7D), but it blocked the effects of NO_2LDL on lamellipodial retraction and retraction fiber formation (Figure 7, D and E; Supplemental Videos 7 and 8). Dynamic movement of membrane and cell velocity were similarly unaffected by NO_2LDL when macrophages were treated with 6-thio-GTP (Figure 7E). The scratch wound migration assay also showed that migration of 6-thio-GTP–treated macrophages was not inhibited by NO_2LDL (Figure 7F). Six-thio-GTP–treated macrophages thus maintained cell polarity and migrating ability despite the presence of NO_2LDL. These studies show that NO_2LDL-induced cytoskeletal changes can be reversed by the blockade of the Vav-Rac interaction.

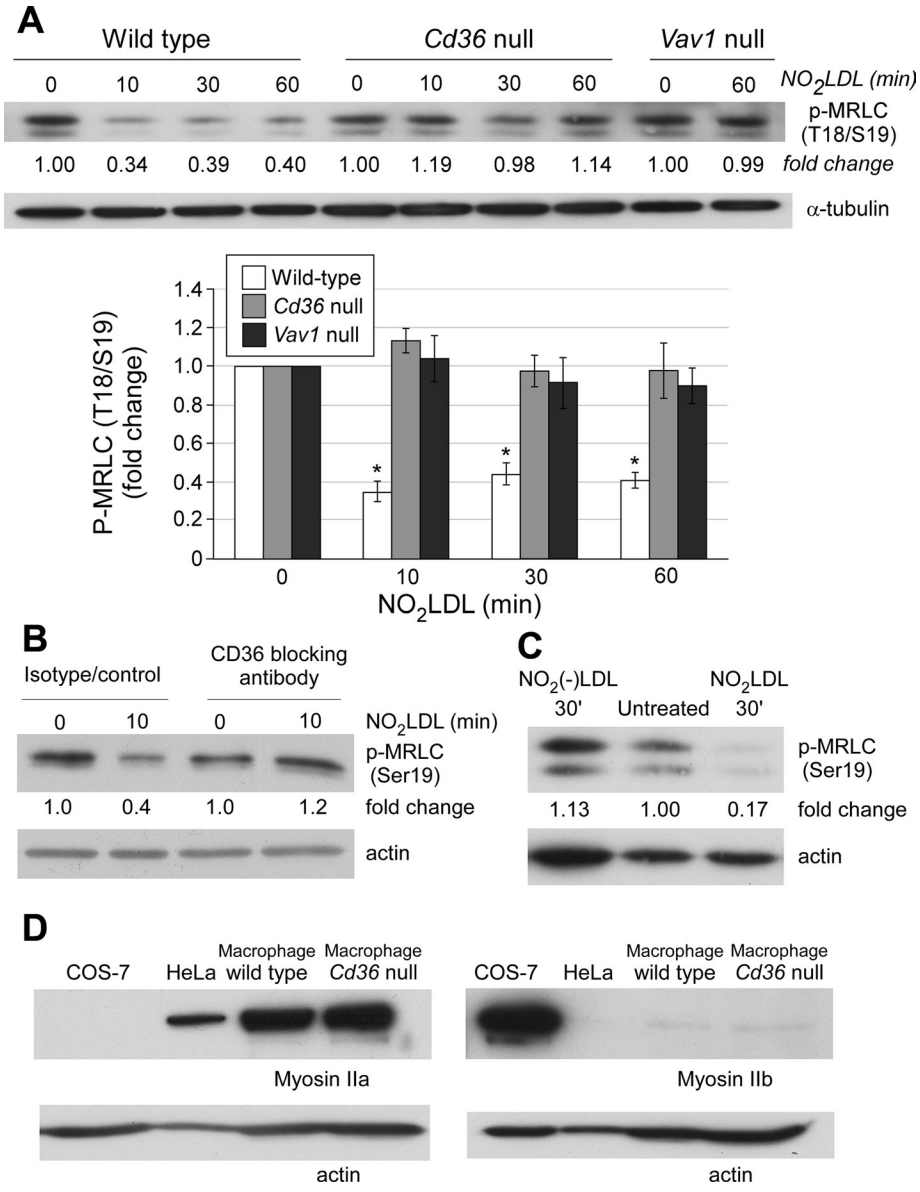

FIGURE 4: OxLDL-CD36 interaction inhibits nonmuscle myosin II activity by dephosphorylating MRLC. (A) *Wt*, *cd36* null, and *vav1* null macrophages were incubated with NO_2LDL at 50 μg/ml for the indicated times and lysed. The lysates were analyzed by Western blot to detect MRLC using an antibody specific for the Thr-18/Ser-19–phosphorylated form. Anti-α-tubulin was used as a loading control. The bar graph shows the fold changes compared with untreated cells (* $p < 0.05$). Data are representative of eight experiments. (B) Human peripheral monocyte–derived macrophages were treated with an isotype control IgG or inhibitory anti-CD36 monoclonal antibody. After incubating with NO_2LDL, macrophages were analyzed as in (A). (C) Phosphorylated MRLC was quantified in macrophages treated with NO_2LDL, NO_2(–)LDL, or medium alone. (D) Myosin IIa (left) and IIb (right) expression was detected in *wt* macrophages, COS-7 cells, and HeLa cells by Western blot. Data are representative of three (B and C) or two (D) experiments.

MLCK inhibition by ML-7 caused loss of cell polarity, similar to the effect of oxLDL

We hypothesized that any pharmacological myosin inhibitor that replicated the signaling effect of NO_2LDL would also induce loss of macrophage cell polarity. ML-7, an MLCK inhibitor that, similar to NO_2LDL, caused decreased phosphorylation of MRLC also induced retraction of front end lamellipodia and loss of polarity when incubated with macrophages (Figures 6B and 8A). However, y27632, a myosin inhibitor that acts by inhibiting ROK, did not induce loss of cell polarity at a concentration that inhibited phosphorylation of MRLC (Figures 6B and 8B). These experiments confirm that inhibition of nonmuscle myosin II by inhibiting MLCK causes loss of macrophage cell polarity.

DISCUSSION

Dysfunctional macrophage migration leading to loss of ability to migrate out of inflammatory microenvironments contributes to the pathogenesis of many important chronic diseases, including obesity and atherosclerosis (Ross, 1999; Glass and Witzum, 2001; Lumeng *et al.*, 2007). These conditions are in contrast to acute inflammation, which resolves in part through inflammatory cell egress. Adipose tissue macrophages in obese/diabetic subjects and macrophages in atherosclerotic plaque share common features. In both settings, macrophages have high intracellular lipid content, and their accumulation is proportionate to the extent of disease (Ross, 1999; Glass and Witzum, 2001; Weisberg *et al.*, 2003; Lumeng *et al.*, 2007; Zeyda and Stulnig, 2007). Importantly, conditions that reverse disease burden are associated with a reduction in the number of macrophages (Weisberg *et al.*, 2003; Clement *et al.*, 2004; Cancello *et al.*, 2005). The molecular mechanisms mediating macrophage "trapping" are incompletely understood. Elegant studies from Randolph and colleagues showed that transplantation of atherosclerotic arterial vessel segments from hyperlipidemic mice into normal mice led to migration of lipid-laden macrophages from plaque to regional lymph nodes and regression of plaque, suggesting that cues from the disease tissue microenvironment undoubtedly play a role in trapping (Llodra *et al.*, 2004). These studies also suggest that targeting the mechanisms responsible for macrophage trapping may lead to a new therapeutic strategy that induces reversal of arterial inflammation.

On the basis of older studies showing that oxLDL inhibits macrophage migration in vitro and that specific forms of oxLDL known to be ligands for the scavenger receptor CD36 are present in obese adipose tissue and advanced atheromatous plaque (Quinn *et al.*, 1987; Nicholson *et al.*, 1995), we hypothesized that interaction of oxLDL with CD36 triggers a signaling cascade that inhibits migration. In support of this hypothesis, we recently demonstrated that oxLDL-mediated inhibition of macrophage migration in vitro and in vivo was dependent on CD36 expression (Park *et al.*, 2009). We defined some of the mechanisms underlying this phenomenon by showing that CD36 signals through src-family kinases and focal adhesion kinase (FAK) to increase actin polymerization and that CD36-dependent generation of intracellular oxidant stress leads to oxidative inactivation of the protein

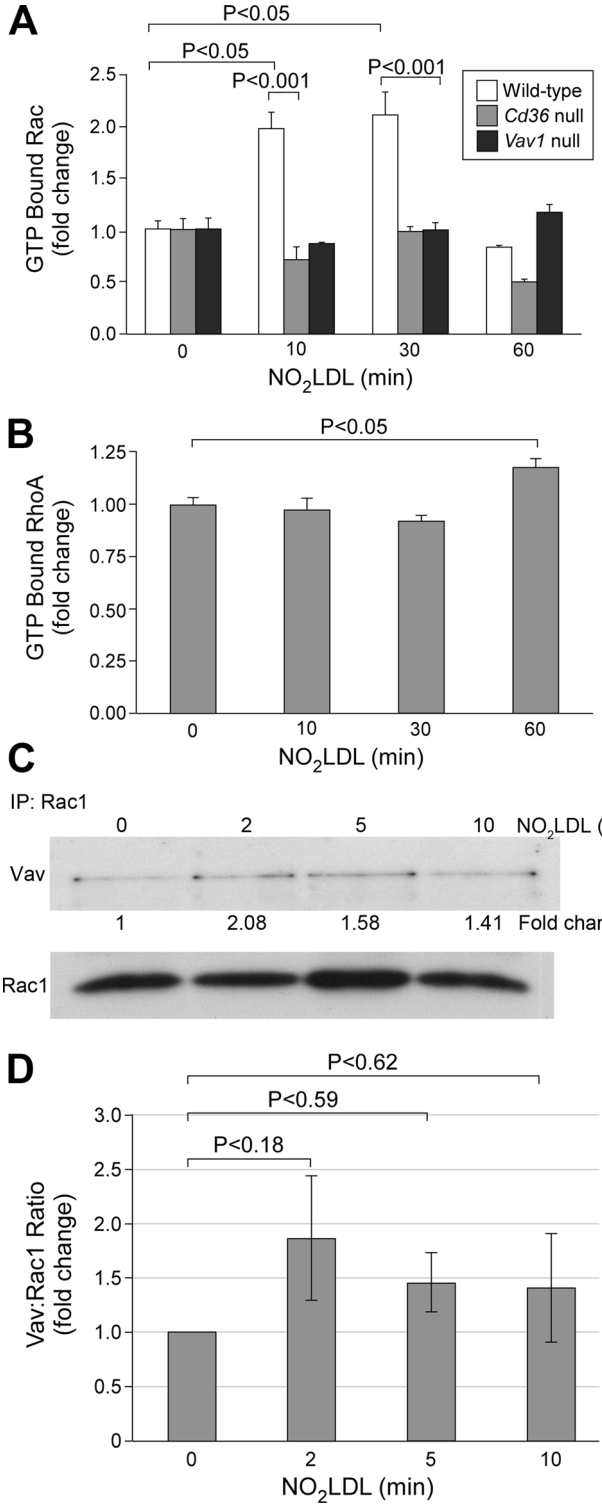

FIGURE 5: OxLDL-CD36 interaction induces Vav-Rac interaction and Rac activation. (A) GTP-bound Rac was measured by ELISA in *wt*, *cd36* null, and *vav1* null macrophages treated with NO_2LDL at 50 μg/ml for the indicated times. (B) GTP-bound Rho was measured by ELISA in *wt* and *Cd36* null macrophages treated as in (A). Data are representative of five (A) or three (B) separate experiments. (C) Rac1 was immunoprecipitated from *wt* macrophages exposed to NO_2LDL for the indicated times. Immunoprecipitates were then analyzed by Western blot with anti-Vav (top) and anti-Rac1 (bottom) monoclonal antibodies. Bar graph shows quantitative analysis of the scanned blots ($n = 3$).

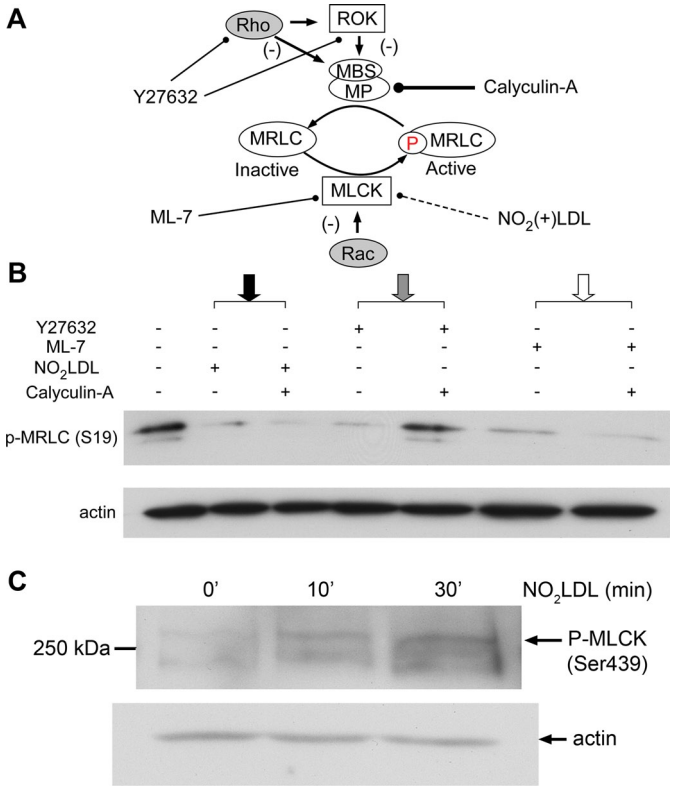

FIGURE 6: OxLDL-induced dephosphorylation of MRLC is not blocked by calyculin-A. (A) Model of the MRLC phosphorylation/dephosphorylation cycles showing points where NO_2LDL and the pharmacologic agents calyculin-A, Y27632, and ML-7 act. Y27632 inhibits myosin through inhibition of Rho and ROK, whereas ML-7 works through MLCK. Calyculin-A inhibits MP and thus reverses the effect of myosin inhibitors that function through Rho or ROK, but not through MLCK. (B) *Wt* macrophages were treated with NO_2LDL at 50 μg/ml followed by treatment with 3 nM calyculin-A, and cell lysates were then examined by Western blot to detect phosphorylated MRLC (Ser-19). To demonstrate that the calyculin-A functioned as predicted, cells were also incubated with 2 μM Y27632 or 12 μM ML-7 and 3 nM calyculin-A and examined as in (B). Data are representative of three experiments. (C) Macrophages from *wt* mice were treated with NO_2LDL as above and examined by Western blot using an antibody specific for the S439-phosphorylated form of MLCK. Data are representative of two experiments.

tyrosine phosphatase responsible for terminating FAK activity. The loss of ability to coordinate actin assembly and disassembly led to enhanced cell spreading and inability to migrate (Park *et al.*, 2009).

We now extend these studies in an important new direction by using live cell imaging to define a previously unknown macrophage signaling pathway involved in regulating cell polarity that is triggered by oxLDL interaction with CD36. Cellular movement starts with the establishment of protrusive forces for membrane extension and traction forces for contraction. (Lauffenburger & Horwitz, 1996). The process of cell polarization has been studied for decades, but the relationship between all participating molecules and their specific roles remains incompletely understood. Small-molecular-weight G proteins including Rho, Rac, and Cdc42 are known to participate (Nobes and Hall, 1999; Wittmann and Waterman-Storer, 2001), and there is abundant evidence that active Rac initiates and maintains directional front end protrusion (Ridley and Hall, 1992; Ridley *et al.*, 1992; Kraynov *et al.*, 2000). In

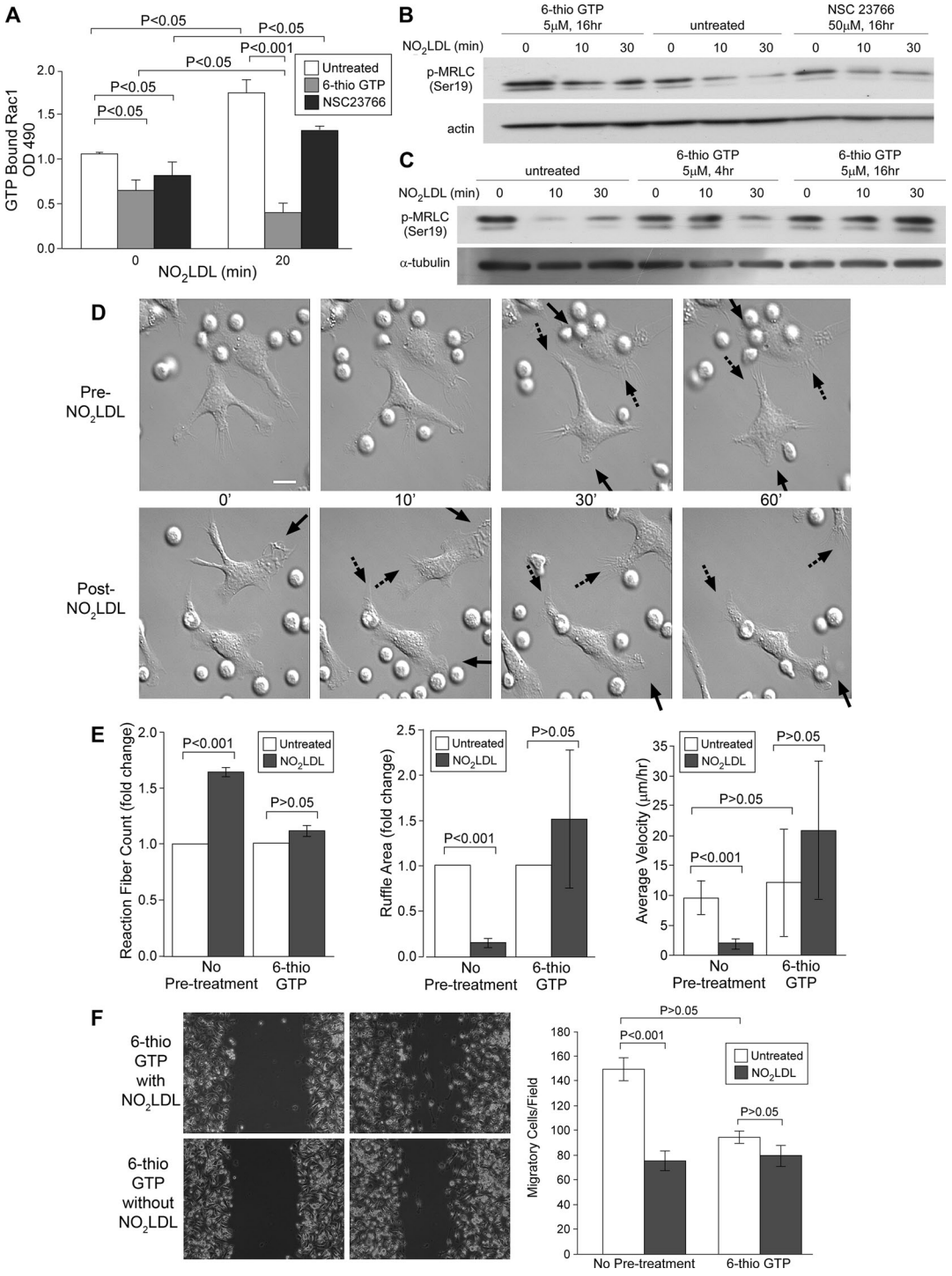

FIGURE 7: Effects of oxLDL on Rac, MRLC, cell polarity, and migration are blocked by 6-thio-GTP. (A) *Wt* macrophages were incubated with 5 μM 6-thio-GTP or 50 μM NSC23766 and treated with NO_2LDL at 50 μg/ml for 20 min. GTP-bound Rac was measured as described in Figure 5. Data are representative of three experiments. (B) Macrophages were treated with 5 μM 6-thio-GTP, 50 μM NSC 23766, or vehicle for 16 h and then exposed to NO_2LDL. Phosphorylated MRLC (S19) was detected by Western blot. Data are representative of two experiments. (C) Macrophages were incubated with 6-thio-GTP for the indicated times and then analyzed for phosphorylated MRLC (S19) as in (C). Data are representative of three experiments. (D) *Wt* macrophages were incubated with 6-thio-GTP or DMSO (for untreated control) and treated with NO_2LDL. Time-lapse images were taken as described in Figure 1. Solid arrows indicate the front end, and dashed arrows indicate the rear end of cells. White scale bar = 10 μm. (E) Retraction fiber counts, ruffle area, and average velocity were calculated as in Figure 2 after exposure to NO_2LDL in the presence or absence of 5 μM 6-thio-GTP. (D and E) Data are representative of three separate experiments analyzing 12 cells. (F) Confluent cell layers of macrophages were pretreated with 6-thio-GTP, scratched, and exposed to NO_2LDL. Bar graphs show migrated cell numbers determined as in Figure 3. Data are representative of three separate experiments, and three randomly chosen fields were recorded by time-lapse microscopy.

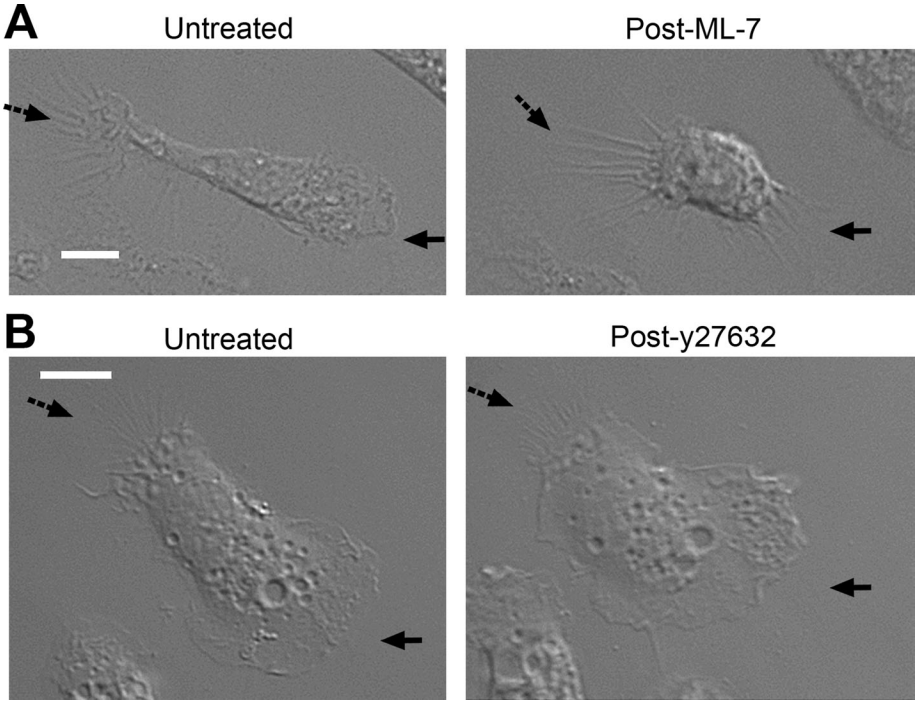

FIGURE 8: MLCK inhibition by ML-7 caused loss of cell polarity, similar to the effect of oxLDL. (A) Resident peritoneal macrophages from *wt* mice were plated onto a serum-coated, glass bottom dish and allowed to spontaneously polarize. Time-lapse images were taken before and after the addition of 12 μM ML-7. (B) Time-lapse images were taken before and after the addition of 2 μM y27632 onto *wt* macrophages as described in (A). (A and B) Solid arrows indicate the front end lamellipodia, and dashed arrows indicate the rear end. Left, representative images taken 40 min after the addition of ML-7 or y27632. White scale bar = 10 μm.

contrast, Rho is more active at the sides and the rear of the cell, antagonizing the function of Rac (Kraynov *et al.*, 2000; Wong *et al.*, 2007). Our data suggest that this simplified view of cell polarity may in fact be incomplete. We showed that activated Rac, induced by oxLDL binding to CD36, breaks cellular asymmetry at the front end by inducing lamellipodial retraction. This effect was driven by Vav-dependent activation of Rac1 with subsequent inhibition of nonmuscle myosin II. Whereas previous studies showed that reduction in myosin-mediated actomyosin contractility induced by RhoA inhibition enhanced retraction of the trailing edge (Omelchenko *et al.*, 2002; Wong *et al.*, 2007), our data showed that Rac1-dependent inhibition of myosin II by oxLDL/CD36 induced retraction at the front end.

Our experiments showed that oxLDL inhibits both random migration and chemotaxis of macrophages by modulating cell polarity, the prerequisite for cellular motility. Asymmetric morphology with defined leading and trailing edges is generated by polarized intracellular signaling that orients protrusion of the front end lamellipodia, integrin-mediated adhesion of the extended membranes, and detachment of the rear end. This sequence of steps, known as the cell motility cycle, occurs in response to a variety of factors. However, it is not clear how this basic motility mechanism is coupled to a steering mechanism that directs cells toward a certain environmental cue and maintains directionally persistent migration. Directional migration has two components: intrinsic cell directionality of migration and external regulation. Cells undergo directed migration when an asymmetric guidance cue such as chemical gradient is presented. The mechanism by which cells maintain directionally persistent migration toward the cues has not been clearly defined. One explanatory mechanism is the "compass model," which proposes that directional sensing couples cellular locomotion by generating new pseudopods (lamellipods) toward the cues (Arrieumerlou and Meyer, 2005). However, a study by Andrew and Insall (2007) contradicts this model by showing evidence that pseudopod generation is controlled independently of chemotactic signaling and directional migration occurs by selecting the most accurately directing preexisting pseudopod. Thus cells bifurcate their pseudopods by suppressing the lateral pseudopods. We have shown that oxLDL/CD36-mediated signaling induced retraction of protrusive lamellipodia and thus inhibited both random and chemotactic migration. In this regard, our data are consistent with the latter model. Because the directing pseudopod is driven from the preexisting pseudopods, inhibition of the random protrusion is predicted to inhibit directional selection of pseudopods for chemotactic movement.

Recent studies have revealed that myosin IIa and IIb have distinct functions (Cai *et al.*, 2006; Chen, 2007). We now show that myosin IIa is the major isoform in macrophages and that it is a critical determinant of cell polarity. Remarkably, retraction of preformed protrusions was induced in polarized macrophages by inactivating myosin II, suggesting that myosin IIa functions in maintaining lamellipodial protrusion and conservation of polarity. Activity of myosin II is regulated by the coordinated activities of Rho and Rac (Zhao and Manser, 2005). Whereas Rho activates myosin II by inhibiting MP (Amano *et al.*, 1996) and/or activating ROK (Kimura *et al.*, 1996; Kawano *et al.*, 1999), the effects of Rac on myosin activity are not clearly defined. Rac activates PAK (del Pozo *et al.*, 2000), but two opposing views on the effect of PAK on MRLC phosphorylation have been published. Some studies report that PAK can phosphorylate MRLC at Ser-19 (Chew *et al.*, 1998), whereas others report that PAK inhibits MLCK activity and decreases phosphorylation of MRLC (Sanders *et al.*, 1999; Goeckeler *et al.*, 2000). It has also been shown that Rac can activate MLCK through a cascade involving extracellular signal-regulated kinase (Robinson and Cobb, 1997). Some of these confounding data may have resulted from the use of overexpression of constitutively active or dominant negative Rac or PAK mutants to probe the system. Our studies, however, took advantage of a natural endogenous receptor-ligand system to modulate the pathway. They showed that oxLDL decreases the activity of myosin II by Rac-mediated inhibition of MRLC phosphorylation by MLCK. Previous studies showing that MLCK regulates MRLC phosphorylation at the cellular periphery while ROK functions at the center of cells (Totsukawa *et al.*, 2000, 2004) are consistent with the live cell imaging demonstrating that oxLDL-induced retraction is localized to the lamellipodial edges (Figure 1; Supplemental Video 2; Supplemental Figure S1). This finding is also supported by our experiments with ML-7, an MLCK inhibitor and y27632, a ROCK inhibitor. ML-7 induced retraction of lamellipodia and loss of macrophage cell polarity as NO_2LDL, but y27632 did not show the

effect at a concentration that decreased MRLC phosphorylation (Figures 6B and 8).

Studies from our lab and others showed that Vav family members are downstream effectors of CD36 signaling (Wilkinson *et al.*, 2006; Rahaman *et al.*, 2011). *Vav* null macrophages have previously been shown to have defects in spreading (Spurrell *et al.*, 2009) and adhesion-induced Rac and Rho activation (Bhavsar *et al.*, 2009), and the cellular responses to oxLDL-induced Vav activation observed in our studies are opposite to these effects, consistent with a critical role for Vav in mediating oxLDL-CD36 cytoskeletal signaling. We found that 6-thio-GTP, a pharmacologic agent that blocks binding of Vav to Rac (Poppe *et al.*, 2006), abrogated oxLDL effects on cell polarity and MRLC phosphorylation. The relevance of Vav to these processes was confirmed by showing that genetic ablation of *Vav1* and *Vav3* in macrophages phenocopied CD36 deficiency with regard to polarity and migration responses to oxLDL. Individual Vav family proteins are known to have both distinct and overlapping functions (Hornstein *et al.*, 2004; Sindrilaru *et al.*, 2009), and indeed we found that Vav3 partially compensates for deficiency of Vav1 in macrophages: *vav1* null cells had delayed and partial response to oxLDL in terms of dynamic membrane movement and cell migration. These effects were blocked by concomitant *vav3* deletion.

Our data provide additional mechanistic support for the proatherogenic role of macrophage CD36 (Febbraio *et al.*, 2000, 2004; Guy *et al.*, 2007; Kuchibhotla *et al.*, 2008) and support a model by which oxLDL/CD36 interactions activate Rac through src-family kinase activation of Vav. Activated Rac then inhibits nonmuscle myosin II by inhibiting phosphorylation of MRLC. Inactivated myosin II cannot generate tension or traction force on lamellipodia resulting in lamellipodial retraction. Lamellipodial retraction leads to a loss of cell polarity, an essential requirement for macrophage migration. Blockade of any step in this process—including CD36 deletion, Vav deletion, or Rac inhibition—prevents the effect of oxLDL and restores macrophage migration. These studies suggest novel ways to promote mobilization of lipid-laden macrophages and induce regression of atherosclerosis. We also suggest that macrophage trapping as a common phenomenon of oxLDL-enriched environments may be a shared target for the treatment of atherosclerosis and adipose tissue inflammation, two major components of metabolic syndrome.

MATERIALS AND METHODS

Reagents and antibodies

LDL prepared from human plasma by density gradient ultracentrifugation (Hatch, 1968) was oxidatively modified by incubation in a buffer containing 50 mM sodium phosphate (pH 7.0) and 100 μM diethylene triamine pentaacetate (DTPA) with 30 nM MPO, 100 μg of glucose, glucose oxidase at 20 ng/ml (grade II; Boehringer Mannheim Biochemicals, Penzberg, Germany), and 0.5 mM $NaNO_2$ at 37°C for 8 h (NO_2LDL) (Podrez *et al.*, 1999). The oxidation reaction was terminated by the addition of 40 μM butylated hydroxyltoluene and 300 nM catalase to the reaction mixture. We also prepared a control LDL termed NO_2(–)LDL, by incubating LDL with all the components mentioned above but $NaNO_2$. Antibodies for phosphorylated MRLC (T18/S19) and phosphorylated MRLC (S19) were purchased from Cell Signaling Technology (Danvers, MA); antibodies for actin and α-tubulin were obtained from Santa Cruz Biotechnology (Santa Cruz, CA); 6-thio-GTP was purchased from Jena Bioscience GmbH (Jena, Germany). COS-7 and HeLa cell lysates, anti-myosin IIa and anti-myosin IIb antibodies, y27632, ML-7, and NSC23766 were generously provided by Thomas Egelhoff, Department of Cell Biology, Cleveland Clinic.

Animals and cells

Vav1 null mice were provided by J. Rivera (National Institutes of Health [NIH], Bethesda, MD), and *Vav1/3* double-null mice were obtained from W. Swat (Washington University School of Medicine, St. Louis, MO). Background-matched mice were used as controls. Resident peritoneal macrophages were collected by lavage and selected by removing unbound cells 30 min after plating onto surfaces devoid of matrix proteins. Thioglycollate-elicited peritoneal macrophages were collected by lavage 4 d after intraperitoneal injection of thioglycollate. Macrophages were cultured in RPMI containing 10% FBS. Human monocytes were isolated from peripheral blood by Ficoll-Hypaque centrifugation and were cultured in RPMI containing human AB serum (10%) for 7 d to allow for macrophage differentiation.

Live cell imaging

Live cell imaging of single cells was performed using TIRF (total internal reflection fluorescence) microscopy (Leica AM TIRF MC System equipped with HCX Plan Apo 100×/1.46 NA Objective Lens; Leica Microsystems, Buffalo Grove, IL). Mouse peritoneal macrophages were plated on a serum-coated glass bottom dish and visualized by transmitted light differential interference contrast imaging. An ImageEM C9100-13 EMCCD camera (Hamamatsu, Shizuoka, Japan) captured an image every 15 s for 1 h before the addition of NO_2LDL and for another 1 h after the addition of NO_2LDL. The same methods were used for evaluating the effects of ML-7 and y27632. Live cell imaging for cell migration assays was performed using a Leica DMIRB inverted microscope with a 100× objective lens (Leica Microsystems).

Cell migration assay

Scratch wound closure migration assay. Peritoneal macrophages from *wt, cd36* null, *vav1* null, or *vav1,3* double-null mice were plated onto glass bottom 6-well or 12-well plates. After 18 h, confluent monolayers were scratched using a pipette tip and rinsed with PBS. RPMI medium was added with or without NO_2LDL. Live cell imaging was used to record the migration of macrophages for 18 h. Images were taken every 5 min and from three randomly chosen locations of each well.

Modified Boyden chamber migration assay. Chemoattractant-directed migration of mouse peritoneal macrophages was measured in a modified Boyden chamber migration assay using Transwell inserts with a 5-μm porous membrane (Corning, Corning, NY). Cells (1.5×10^5) were loaded into the migration chamber with or without lipoproteins including NO_2(–)LDL and NO_2LDL. Medium containing MCP-1 at 20 ng/ml was placed in some of the lower chambers. After allowing cell migration for 16 h, cells were removed from the upper side of membranes, and nuclei of migratory cells on the lower side of the membrane were stained with 4′,6-diamidino-2-phenylindole (DAPI). The number of migratory cells was counted by fluorescence microscopy (100× magnification).

Image analysis

Microscopic images were analyzed by Image-Pro Plus software (Media Cybernetics, Bethesda, MD). Retraction fibers around the front end lamellipodia were marked in color and counted, as were the ruffle areas as parameters to evaluate dynamic membrane movement. Ruffle area was defined as instant protrusive area from the prior cellular margin taken 15 s earlier. The protrusive areas were counted every 15 s for 1 h before and after the addition of NO_2LDL.

Pictures from live cell imaging were merged and video clips generated using the software.

Western blot analysis

Mouse peritoneal macrophages incubated with NO_2LDL or NO_2(–) LDL at 50 μg/ml for the indicated times were lysed with sample buffer containing 4% SDS after treating the cells with 10% TCA. Lysates were separated by SDS–PAGE and transferred to PVDF membranes (Millipore, Billerica, MA). Membranes were probed with antibodies against phosphorylated MRLC, actin, or α-tubulin for normalization. Band intensities were quantified by ImageJ (http://rsbweb.nih.gov/ij) and Gel-Pro Analyzer (Media Cybernetics). Immunoblotting for nonmuscle myosin IIa and IIb was performed as described earlier in text using anti-myosin IIa and anti-myosin IIb antibodies. COS-7 and HeLa cell lysates served as positive or negative controls for myosin IIa or IIb.

Immunoprecipitation

Mouse peritoneal macrophages were lysed in buffer consisting of 20 mM Tris-HCl (pH 7.5), 150 mM NaCl, 1 mM EDTA, 1 mM EGTA, 1% Triton X-100, 2.5 mM sodium pyrophosphate, 1 mM β-glycerophosphate, and 1 mM sodium orthovanadate. Cell lysates were added to protein A/G sepharose beads (Santa Cruz Biotechnology), conjugated with anti-Rac antibody (abcam, Cambridge, MA), and incubated overnight at 4°C. The sepharose beads were rinsed, resuspended in 2X Laemmli sample buffer (Bio-Rad, Hercules, CA), and heated at 100°C. After centrifugation, the supernatants were loaded onto SDS–PAGE gels and transferred to PVDF membrane. Immunoblotting for Vav was performed, and Exacta-Cruz C (Santa Cruz Biotechnology) was used for detection.

Rac and RhoA activity assay

GTP-bound Rac and RhoA were detected by a G-LISA Rac activation assay kit and a G-LISA RhoA activation assay kit from Cytoskeleton (Denver, CO). For these assays, mouse peritoneal macrophages treated with or without NO_2LDL were lysed. Cell lysate protein (5–10 μg) was applied to a 96-well plate coated with the p21 binding domain of PAK or the Rho binding domain of Rhotekin, both of which are known to specifically bind to GTP-bound Rac and RhoA, respectively (Burbelo *et al.*, 1995). After a 30-min incubation, the plates were rinsed and anti-Rac or anti-RhoA antibody was added. Horseradish peroxidase-conjugated secondary antibody was added 1 h later, and the level of antibody binding was determined by a colorimetric method.

ACKNOWLEDGMENTS

This work was supported by NIH grant P01HL087018 to R.L.S.We gratefully acknowledge Josephine Adams at the University of Bristol and Alan Tartakoff at Case Western Reserve University for their advice on the live cell imaging. This work was submitted in partial fulfillment of the requirements for a PhD degree in Cell Biology from Case Western Reserve University (Y.M.P.).

REFERENCES

Amano M, Ito M, Kimura K, Fukata Y, Chihara K, Nakano T, Matsuura Y, Kaibuchi K (1996). Phosphorylation and activation of myosin by Rho-associated kinase (Rho-kinase). J Biol Chem 271, 20246–20249.

Andrew N, Insall RH (2007). Chemotaxis in shallow gradients is mediated independently of PtdIns 3-kinase by biased choices between random protrusions. Nat Cell Biol 9, 193–200.

Arrieumerlou C, Meyer T (2005). A local coupling model and compass parameter for eukaryotic chemotaxis. Dev Cell 8, 215–227.

Bhavsar PJ, Vigorito E, Turner M, Ridley A (2009). Vav GEFs regulate macrophage morphology and adhesion-induced Rac and Rho activation. Exp Cell Res 315, 3345–3358.

Burbelo PD, Dreschsel D, Hall A (1995). A conserved binding motif defines numerous candidate target proteins for both Cdc42 and Rac GTPases. J Biol Chem 270, 29071–29074.

Cai Y *et al.* (2006). Nonmuscle myosin IIA-dependent force inhibits cell spreading and drives F-actin flow. Biophys J 91, 3907–3920.

Cancello R *et al.* (2005). Reduction of macrophage infiltration and chemoattractant gene expression changes in white adipose tissue of morbidly obese subjects after surgery-induced weight loss. Diabetes 54, 2277–2286.

Charest PG, Firtel RA (2007). Big roles for small GTPases in the control of directed cell movement. Biochem J 401, 377–390.

Chen CS (2007). Separate but not equal: differential mechanical roles for myosin isoforms. Biophys J 92(9), 2984–2985.

Chew TL, Masaracchia RA, Goeckeler ZM, Wysolmerski RB (1998). Phosphorylation of non-muscle myosin II regulatory light chain by p21-activated kinase (PAK). J Muscle Res Cell Motil 19, 839–854.

Chung CY, Lee S, Briscoe C, Ellsworth C, Firtel RA (2000). Role of Rac in controlling the actin cytoskeleton and chemotaxis in motile cells. Proc Natl Acad Sci USA 97, 5225–5230.

Clement K *et al.* (2004). Weight loss regulates inflammation-related genes in white adipose tissue of obese subjects. FASEB J 18, 1657–1669.

Daoud AS, Jarmolych J, Augustyn JM, Fritz KE (1981). Sequential morphologic studies of regression of advanced atherosclerosis. Arch Pathol Lab Med 105, 233–239.

del Pozo MA, Price LS, Alderson NB, Ren XD, Schwartz MA (2000). Adhesion to the extracellular matrix regulates the coupling of the small GTPase Rac to its effector PAK. EMBO J 19, 2008–2014.

Dumontier M, Hocht P, Mintert U, Faix J (2000). Rac1 GTPases control filopodia formation, cell motility, endocytosis, cytokinesis and development in Dictyostelium. J Cell Sci 113, 2253–2265.

Fazal F *et al.* (2005). Inhibiting myosin light chain kinase induces apoptosis in vitro and in vivo. Mol Cell Biol 25, 6259–6266.

Febbraio M, Guy E, Silverstein RL (2004). Stem cell transplantation reveals that absence of macrophage CD36 is protective against atherosclerosis. Arterioscler. Thromb Vasc Biol 24, 2333–2338.

Febbraio M, Podrez EA, Smith JD, Hajjar DP, Hazen SL, Hoff HF, Sharma K, Silverstein RL (2000). Targeted disruption of the class B scavenger receptor CD36 protects against atherosclerotic lesion development in mice. J Clin Invest 105, 1049–1056.

Gao Y, Dickerson JB, Guo F, Zheng J, Zheng Y (2004). Rational design and characterization of a Rac GTPase-specific small molecule inhibitor. Proc Natl Acad Sci USA 101, 7618–7623.

Glass C, Witzum J (2001). Atherosclerosis, the road ahead. Cell 104, 503–516.

Goeckeler ZM, Masaracchia RA, Zeng Q, Chew TL, Gallagher P, Wysolmerski RB (2000). Phosphorylation of myosin light chain kinase by p21-activated kinase PAK2. J Biol Chem 275, 18366–18374.

Guy E, Kuchibhotla S, Silverstein RL, Febbraio M (2007). Continued inhibition of atherosclerotic lesion development in long term Western diet fed $CD36^0$/$apoE^0$ mice. Atherosclerosis 192, 123–130.

Hatch FT (1968). Practical methods for plasma lipoprotein analysis. Adv Lipid Res 6, 1–68.

Hornstein I, Alcover A, Katzav S (2004). Vav proteins, masters of the world of cytoskeleton organization. Cell Signal 16, 11–11.

Ikebe M, Hartshorne DJ (1985). Phosphorylation of smooth muscle myosin at two distinct sites by myosin light chain kinase. J Biol Chem 260, 10027–10031.

Ikebe M, Hartshorne DJ, Elzinga M (1986). Identification, phosphorylation, and dephosphorylation of a second site for myosin light chain kinase on the 20,000-dalton light chain of smooth muscle myosin. J Biol Chem 261, 36–39.

Ikebe M, Koretz J, Hartshorne DJ (1988). Effects of phosphorylation of light chain residues threonine 18 and serine 19 on the properties and conformation of smooth muscle myosin. J Biol Chem 263, 6432–6437.

Ito M, Nakano T, Erdodi F, Hartshorne DJ (2004). Myosin phosphatase: structure, regulation and function. Mol Cell Biochem 259, 197–209.

Kato Y, Fusetani N, Matsunaga S, Hashimoto K (1986). Calyculin A, a novel antitumor metabolite from the marine sponge Discodermia calyx. J Am Chem Soc 108, 2780–2781.

Kawano Y, Fukata Y, Oshiro N, Amano M, Nakamura T, Ito M, Matsumura F, Inagaki M, Kaibuchi K (1999). Phosphorylation of myosin-binding subunit (MBS) of myosin phosphatase by Rho-kinase in vivo. J Cell Biol 147, 1023–1038.

Kimura K *et al*. (1996). Regulation of myosin phosphatase by Rho and Rho-associated kinase (Rho-kinase). Science 273, 245–248.
Kraynov VS, Chamberlain C, Bokoch GM, Schwartz MA, Slabaugh S, Hahn KM (2000). Localized Rac activation dynamics visualized in living cells. Science 290, 333–337.
Kuchibhotla S, Vanegas D, Kennedy DJ, Guy E, Nimako G, Morton RE, Febbraio M (2008). Absence of CD36 protects against atherosclerosis in ApoE knock-out mice with no additional protection provided by absence of scavenger receptor A I/II. Cardiovasc Res 78, 185–196.
Lauffenburger DA, Horwitz AF (1996). Cell migration: a physically integrated molecular process. Cell 84, 359–369.
Lei M., Lu W, Meng W, Parrini MC, Eck MJ, Mayer BJ, Harrison SC (2000). Structure of PAK1 in an autoinhibited conformation reveals a multistage activation switch. Cell 102, 3387–397.
Llodra J, Angeli V, Liu J, Trogan E, Fisher EA, Randolph GJ (2004). Emigration of monocyte-derived cells from atherosclerotic lesions characterizes regressive, but not progressive, plaques. Proc Natl Acad Sci USA 101, 11779–11784.
Lumeng CN, Deyoung SM, Bodzin JL, Saltiel AR (2007). Increased inflammatory properties of adipose tissue macrophage recruited during diet-induced obesity. Diabetes 56, 16–23.
Nicholson AC, Frieda S, Pearce A, Silverstein RL (1995). Oxidized LDL binds to CD36 on human monocyte-derived macrophages and transfected cell lines. Evidence implicating the lipid moiety of the lipoprotein as the binding site. Arteriosc Thromb Vasc Biol 15, 269–275.
Nobes CD, Hall A (1999). Rho GTPases control polarity, protrusion, and adhesion during cell movement. J Cell Biol 144, 1235–1244.
Omelchenko T, Vasiliev JM, Gelfand IM, Feder HH, Bonder EM (2002). Mechanisms of polarization of the shape of fibroblasts and epithelio-cytes: separation of the roles of microtubules and Rho-dependent actin–myosin contractility. Proc Natl Acad Sci USA 99, 10452–10457.
Pankov R, Endo Y, Even-Ram S, Araki M, Clark K, Cukierman E, Matsumoto K, Yamada KM (2005). A Rac switch regulates random versus directionally persistent cell migration. J Cell Biol 170, 793–802.
Parent CA, Devreotes PN (1999). A cell's sense of direction. Science 284, 765–770.
Park YM, Febbraio M, Silverstein RL (2009). CD36 modulates migration of mouse and human macrophages in response to oxidized LDL and may contribute to macrophage trapping in the arterial intima. J Clin Invest 119, 136–145.
Phillips HM, Murdoch JN, Chaudhry B, Copp AJ, Henderson DJ (2005). *Vang12* acts via RhoA signaling to regulate polarized cell movements during development of the proximal outflow tract. Circ Res 96, 292–299.
Podrez EA, Schmitt D, Hoff HF, Hazen SL (1999). Myeloperoxidase-generated reactive nitrogen species convert LDL into an atherogenic form in vitro. J Clin Invest 103, 111547–1560.
Poppe D *et al*. (2006). Azathioprine suppresses ezrin-radixin-moesin-dependent T Cell-APC conjugation through inhibition of Vav guanosine exchange activity on Rac proteins. J Immunol 176, 640–651.
Quinn MT, Parthasarathy S, Fong LG, Steinberg D (1987). Oxidatively modified low density lipoproteins: a potential role in recruitment and retention of monocyte/macrophages during atherogenesis. Proc Natl Acad Sci USA 84, 2995–2998.
Raftopoulou M, Hall A (2004). Cell migration: Rho GTPases lead the way. Dev Biol 265, 23–32.
Rahaman SO, Lennon DJ, Febbraio M, Podrez EA, Hazen SL, Silverstein RL (2006). A CD36-dependent signaling cascade is necessary for macrophage foam cell formation. Cell Metab 4, 211–221.
Rahaman SO, Swat W, Febbraio M, Silverstein RL (2011). Vav family Rho guanine nucleotide exchange factors regulate CD36-mediated macrophage foam cell formation. J Biol Chem 286, 7010–7017.
Ridley AJ, Hall A (1992). The small GTP-binding protein rho regulates the assembly of focal adhesions and stress fibers in response to growth factors. Cell 70, 389–399.
Ridley AJ, Paterson HF, Johnston CL, Diekmann D, Hall A (1992). The small GTP-binding protein Rac regulates growth factor-induced membrane ruffling. Cell 70, 401–410.
Ridley AJ, Schwartz MA, Burridge K, Firtel RA, Ginsberg MH, Borisy G, Parsons JT, Horwitz AR (2003). Cell migration: integrating signals from front to back. Science 302, 1704–1709.
Robinson MJ, Cobb MH (1997). Mitogen-activated protein kinase pathways. Curr Opin Cell Biol 9, 180–186.
Ross R (1999). Atherosclerosis-an inflammatory disease. N Engl J Med 340, 115–126.
Sander EE, ten Klooster JP, van Delft R, van Delft S, der Kammen RA, Collard JG (1999). Rac downregulates Rho activity: reciprocal balance between both GTPases determines cellular morphology and migratory behavior. J Cell Biol 147, 1009–1022.
Sanders LC, Matsumura F, Bokoch GM, de Lanerolle P (1999). Inhibition of myosin light chain kinase by p21-activated kinase. Science 283, 2083–2085.
Shabir S., Borisova L, Wray S, Burdyga T (2004). Rho-kinase inhibition and electromechanical coupling in rat and guinea-pig ureter smooth muscle: Ca^{2+}-dependent and -independent mechanisms. J Physiol 560, 839–855.
Simons M, Wang M, McBride OW, Kawamoto S, Yamasaki K, Gdula D, Adelstein RS, Weir L (1991). Human nonmuscle myosin heavy chains are encoded by two genes located on different chromosomes. Circ Res 69, 530–539.
Sindrilaru A *et al*. (2009). Wound healing defect of *Vav3*$^{-/-}$ mice due to impaired β_2-integrin–dependent macrophage phagocytosis of apoptotic neutrophils. Blood 113, 5266–5276.
Somlyo AP, Somlyo AV (2003). Ca^{2+} sensitivity of smooth muscle and nonmuscle myosin II: modulated by G proteins, kinases, and myosin phosphatase. Physiol Rev 83, 1325–1358.
Spurrell DR, Luckashenak NA, Minney DC, Chaplin A, Penninger JM, Liwski RS, Clements JL, West KA (2009). Vav1 regulates the migration and adhesion of dendritic cells. J Immunol 183, 310–318.
Takai A, Bioalojan C, Troschka M, Ruegg JC (1987). Smooth muscle myosin phosphatase inhibition and force enhancement by black sponge toxin. FEBS Lett 217, 81–84.
Totsukawa G, Wu Y, Sasaki Y, Hartshorne DJ, Yamakita Y, Yamashiro S, Matsumura F (2004). Distinct roles of MLCK and ROCK in the regulation of membrane protrusions and focal adhesion dynamics during cell migration of fibroblasts. J Cell Biol 164, 3427–439.
Totsukawa G, Yamakita Y, Yamashiro S, Hartshorne DJ, Sasaki Y, Matsumura F (2000). Distinct roles of ROCK (Rho-kinase) and MLCK in spatial regulation of MLC phosphorylation for assembly of stress fibers and focal adhesions in 3T3 fibroblasts. J Cell Biol 150, 4797–806.
van Leeuwen FN, van Delft S, Kain HE, der Kammen RA, Collard JG (1999). Rac regulates phosphorylation of myosin-II heavy chain, actomyosin disassembly and cell spreading. Nat Cell Biol 1, 242–248.
Vicente-Manzanares M, Sánchez-Madrid F (2004). Role of the cytoskeleton during leukocyte responses. Nat Rev Immunol 4, 110–122.
Vicente-Manzanares M, Zareno J, Whitmore L, Choi CK, Horwitz AF (2007). Regulation of protrusion, adhesion dynamics and polarity by myosins IIA and IIB in migrating cells. J Cell Biol 176, 573–580.
Weisberg S, McCann D, Desai M, Rosenbaum M, Leibel R, Ferrante A (2003). Obesity is associated with macrophage accumulation in adipose tissue. J Clin Invest 112, 1796–1808.
Wells CM, Bhavsar PJ, Evans IR, Vigorito E, Turner M, Tybulewicz V, Ridley AJ (2005). Vav1 and Vav2 play different roles in macrophage migration and cytoskeletal organization. Exp Cell Res 310, 303–310.
Wilkinson B, Koenigsknecht-Talboo J, Grommes C, Lee CY, Landreth G (2006). Fibrillar beta-amyloid-stimulated intracellular signaling cascades require Vav for induction of respiratory burst and phagocytosis in monocytes and microglia. J Biol Chem 281, 3020842–20850.
Wittmann T, Waterman-Storer CM (2001). Cell motility: can Rho GTPases and microtubules point the way? J Cell Sci 114, 3795–3803.
Wong K, van Keymeulen A, Bourne HR (2007). PDZRhoGEF and myosin II localize RhoA activity to the back of polarizing neutrophil-like cells. J Cell Biol 179, 1141–1148.
Yamaguchi Y, Katoh H, Yasui H, Mori K, Negishi M (2001). RhoA inhibits the nerve growth factor-induced Rac1 activation through Rho-associated kinase-dependent pathway. J Biol Chem 276, 18977–18983.
Zeyda M, Stulnig TM (2007). Adipose tissue macrophages. Immunol Lett 112, 61–67.
Zhao Z, Manser E (2005). PAK and other Rho-associated kinases-effectors with surprisingly diverse mechanisms of regulation. Biochem J 386, 210–214.
Zigmond SH, Levitsky HI, Kreel BJ (1981). Cell polarity: an examination of its behavioral expression and its consequences for polymorphonuclear leukocyte chemotaxis. J Cell Biol 89, 585–592.